Electric and thermoelectric phenomena in a multilevel quantum dot attached to ferromagnetic electrodes

M. Wierzbicki and R. Świrkowicz
Faculty of Physics, Warsaw University of Technology, ul. Koszykowa 75, 00-662 Warsaw, Poland
(Received 12 July 2010; published 28 October 2010)

Nonequilibrium Green's function formalism is used to study electron and energy transport in the Coulomb-blockade regime through a two-level quantum dot/molecule attached to ferromagnetic leads. Interplay between magnetic and thermoelectric properties is investigated in the nonlinear-response regime and strong spin effects in the nonlinear thermopower are found. Significant spin thermopower S_{spin} can be generated in a relatively wide region of temperature difference ΔT. It is also shown that spin asymmetry due to presence of one half-metallic and one nonmagnetic electrodes plays an important role and strongly influences both charge and spin thermopower. S_{spin} varies considerably, if the roles of both leads are interchanged. Spin thermopower is enhanced in the region of higher values of ΔT, if half-metallic electrode acts as an energy drain. On the other hand, in such a configuration, Pauli spin blockade occurs in electron transport.

DOI: 10.1103/PhysRevB.82.165334 PACS number(s): 73.23.Hk, 73.50.Lw, 85.80.Fi

I. INTRODUCTION

Recently, thermoelectric phenomena in nanostructure systems have been intensively studied both experimentally and theoretically.[1–5] In particular, a new field of research, focused on spin effects in energy transport has been developed in view of future application in spintronic devices.[6–17] Spin-dependent heat current was experimentally investigated in magnetic multilayer nanowires.[7,8] Magnetothermoelectric power (MTEP) was measured, as well as magnetothermogalvanic voltage was determined, which describes ac voltage response to a small temperature oscillations in a presence of dc current. A strong dependence on spin asymmetry was found. "Three-current model," which joins heat current and charge currents in two spin channels corresponding to spins up and down, was developed to discuss the experimental data.[7] Spin Seebeck effect was also observed for a ferromagnetic slab and spin voltage generated by temperature gradient was measured.[9] It was theoretically shown that in ferromagnetic tunnel junctions thermal conductance and Peltier effect vary with configuration of magnetic moments.[10] Moreover, at low temperatures, a strong suppression of electrical and thermal currents was observed for antiparallel orientation of magnetizations. With use of finite-element theory a significant dependence of thermal coefficients on relative alignment of magnetic moments was also obtained for magnetic multilayer nanostructures.[11] Spin-transfer torque due to a flow of spin-polarized heat current through a multilayer system was found, which indicates that current-induced magnetization switching can be affected by thermal phenomena.[12] Moreover, very recently, with use of scattering theory, domain-wall dynamics has been studied in a presence of temperature gradient and thermally induced motion of the walls has been observed.[13]

Thermoelectric properties of nanoscale systems containing quantum dots (QDs) are strongly influenced both by quantum confinement and Coulomb-blockade effect, which lead to distinct phenomena like oscillations of thermal coefficients with gate voltage.[18–21] Additional fine structure due to discrete levels was found for small dots.[22] It is also worth noting that experiments performed on QDs in the Kondo regime reveal that thermopower is strongly influenced by spin correlations.[23] Interplay between spin effects and thermal transport through a single-level QD attached to ferromagnetic leads was also studied.[16,17] The investigations reveal a significant dependence of thermal coefficients on spin-polarization factor in electrodes as well as on the relative orientation of magnetic moments.[17] Spin Seebeck effect and spin-dependent thermal efficiency, described by the spin-dependent figure of merit was also discussed.[16,17] Studies of the thermal properties of strongly correlated QD attached to ferromagnetic leads were also performed in the Kondo regime.[15] It was found that thermopower, calculated for parallel configuration of magnetic moments, is strongly suppressed at low temperatures due to splitting of the Kondo resonance. It should be pointed out that all these calculations, performed in the Coulomb blockade and in Kondo regime, correspond to the linear-response region only.

To study transport phenomena in systems subject to considerable voltage and temperature gradient, a more general approach is required, which allows to describe nonlinear effects. Various methods were developed to investigate charge transport for a variety of systems in the nonlinear regime. In particular, Pauli spin-blockade effects in two coupled QDs, asymmetrically attached to ferromagnetic electrodes were investigated in the sequential tunneling approximation with use of density-matrix approach[24–26] as well as in the cotunneling regime.[27] Diagrammatic technique was also used to study spin blockade in a two-level QD attached to one half-metallic ferromagnet (HMF) and one nonmagnetic (NM) electrodes.[28] It is worth noting that very recently, in a semiconductor QD attached to one FM and one NM electrodes negative differential conductance (NDC) has been experimentally observed for both forward- and reverse-bias voltages.[29] When electrons tunnel from NM electrode to FM one the Pauli spin-blockade effect occurs but for the reverse bias a different mechanism can be expected.

Thermal phenomena in the nonlinear transport through QD were mainly investigated for nonmagnetic systems, in which spin effects are irrelevant.[30–35] Some investigations

were also performed for the Kondo regime.[34] The nonlinear thermoelectric properties of molecular junctions are of special interest. First of all, strong nonlinearity was observed experimentally in organic molecules.[3] Moreover, it was shown that optimal thermoelectric operation of the molecular device can be achieved in the nonlinear, nonequilibrium regime.[35] Additional advantage of molecular systems is that the corresponding phonon contributions to thermal properties may be small.[3,36] In particular, such contributions to heat current become negligible when tunnel coupling to the leads is symmetric and larger than phonon couplings.[35]

Here, we present studies of spin-dependent phenomena in the nonlinear transport through a two-level QD/molecule in the Coulomb-blockade regime, based on the nonequilibrium Green's function formalism. The analysis may also hold for two electrostatically coupled QDs. Similar approach was used in our previous work to investigate thermoelectric properties of nonmagnetic system in the linear-response regime.[37] In the present paper we focus on the spin-related phenomena in the nonlinear charge transport and thermopower. The approach allows us to study blockade effects in the charge transport and to show that in junctions with strong spin asymmetry, in which one of the levels is weakly coupled to HMF and NM electrodes, negative differential conductance can be observed for both polarizations of bias voltage.

Furthermore, spin effects in the nonlinear thermopower are discussed. Up to now, in the Coulomb-blockade region spin-dependent thermoelectric phenomena were mainly investigated for a single-level dot within the linear-response regime,[16,17] though some preliminary results obtained in nonlinear regime were also presented.[17] Here, we show that in a wide region of temperature difference between electrodes a significant spin thermopower can be generated. In particular, a considerable and practically constant spin thermopower can be observed in the wide region of ΔT for junctions with strong spin asymmetry, which show Pauli spin blockade in charge transport.

The paper is organized as follows. In Sec. II the model is presented and the transmission expressed in terms of Green's functions is given. Charge current flowing in the system due to bias voltage applied is discussed in Sec. III whereas results obtained for thermopower in a presence of temperature gradient are discussed in Sec. IV. Final conclusions and summary are given in Sec. V.

II. MODEL

System under consideration, composed of a multilevel quantum dot/molecule attached to ferromagnetic leads, is described by the following Hamiltonian: $H=H_D+H_e+H_T$. The first term H_D corresponds to the dot and is taken in the form

$$H_D=\sum_{j\sigma}\varepsilon_j d_{j\sigma}^{+}d_{j\sigma}+\frac{1}{2}\sum_{ij\sigma\sigma'}U_{ij}d_{i\sigma}^{+}d_{i\sigma}d_{j\sigma'}^{+}d_{j\sigma'}, \tag{1}$$

where $\varepsilon_j=\varepsilon_{j0}+V_g$ is the energy of the level j which can be shifted by the gate voltage V_g. U_j and U_{ij} describe intralevel and interlevel Coulomb correlations, respectively. $d_{j\sigma}^{+}$ ($d_{j\sigma}$) represents creation (annihilation) operator of electron in the state $j\sigma$. The term $H_e=\Sigma_{\beta=L,R,k\sigma}\varepsilon_{k\beta\sigma}c_{k\beta\sigma}^{+}c_{k\beta\sigma}$ corresponds to the noninteracting electrons in the left ($\beta=L$) and right ($\beta=R$) leads whereas $H_T=\Sigma_{\beta kj\sigma}(V_{kj\sigma}^{\beta}c_{k\beta\sigma}^{+}d_{j\sigma}+V_{kj\sigma}^{*\beta}d_{j\sigma}^{+}c_{k\beta\sigma})$ describes tunneling effects between the dot and electrodes. $V_{kj\sigma}^{\beta}$ are elements of the tunneling matrix corresponding to the level j and $c_{k\beta\sigma}^{+}$ ($c_{k\beta\sigma}$) denotes creation (annihilation) operator of electron with wave vector k and spin σ in β electrode.

In general, electrochemical potential of the lead β with temperature T_β can be spin dependent, as temperature gradient can generate spin-dependent voltage.[9] Thereby, we assume that electrochemical potentials of left and right electrodes are equal to: $\mu_{L\sigma}=\mu_0+\frac{1}{2}V_\sigma$, $\mu_{R\sigma}=\mu_0-\frac{1}{2}V_\sigma$, respectively. V_σ includes the charge and spin voltages and μ_0 corresponds to the Fermi energy of the system in equilibrium. The charge and spin currents $I=I_\uparrow+I_\downarrow$, $I_{spin}=\hbar/e(I_\uparrow-I_\downarrow)$ can be introduced and I_σ denotes here the current flowing in a channel corresponding to spin σ.

The calculate current I_σ we apply nonequilibrium Green's function formalism based on the equation-of-motion method. Introducing retarded G^r (advanced G^a) and lesser $G^<$ Green's functions one obtains the following expression:[38,39]

$$I_\sigma=i\frac{e}{2\hbar}\int\frac{dE}{2\pi}\sum_j\{[\Gamma_{j\sigma}^{L}f_{L\sigma}(E)-\Gamma_{j\sigma}^{R}f_{R\sigma}(E)][G_{j\sigma}^{r}(E)-G_{j\sigma}^{a}(E)]+(\Gamma_{j\sigma}^{L}-\Gamma_{j\sigma}^{R})G_{j\sigma}^{<}(E)\}, \tag{2}$$

where $f_{\beta\sigma}=[\exp(E-\mu_{\beta\sigma})/kT_\beta+1]^{-1}$ is the Fermi-Dirac distribution function in the β electrode and $G^{r(a<)}(E)$ represents the Fourier transform of the appropriate Green's function. $\Gamma_{j\sigma}^{\beta}=\Gamma_j(1+\hat{\sigma}p_\beta)$ determines here the spin-dependent coupling strength of the dot level j with electrode β, p_β is related to the lead's polarization and $\hat{\sigma}=1$ for spin index $\sigma=\uparrow$ or $\hat{\sigma}=-1$ for $\sigma=\downarrow$. Γ_j denotes the coupling strength of the level j with electrodes and is treated as a parameter independent of energy.

Green's function $G_{j\sigma}^{r}=\langle\langle d_{j\sigma},d_{j\sigma}^{+}\rangle\rangle$ is calculated with use of procedure proposed by Chang and Kuo[40,41] based on the equation-of-motion method. Following the procedure, justified in the Coulomb-blockade regime, one can express G^r in the form (for details see Ref. 40)

$$G_{j\sigma}^{r}(E)=\sum_{k=0}^{2}p_k\left(\frac{1-N_{j-\sigma}}{E-\varepsilon_j-A_k-\Sigma_j^{r}}+\frac{N_{j-\sigma}}{E-\varepsilon_j-U_j-A_k-\Sigma_j^{r}}\right). \tag{3}$$

The summation is over possible configurations in which level l, different from j, is occupied by zero, one or two particles, respectively. p_k denotes here the probability factor of a particular configuration k and is expressed in terms of the average one-particle $N_{l\sigma}=\langle n_{l\sigma}\rangle=\langle d_{l\sigma}^{+}d_{l\sigma}\rangle$ and two-particle $\langle n_{l-\sigma}n_{l\sigma}\rangle$ occupation numbers. A_k in the last equation denotes the sum of all interactions seen by the electron in the level j due to other particles occupying the level l in configuration k and expressed in terms of U_{jl}.[40] The occupation numbers are expressed in terms of lesser Green's functions: $N_{l\sigma}=-i\int dE/2\pi\langle\langle d_{l\sigma},d_{l\sigma}^{+}\rangle\rangle^{<}$, $\langle n_{l\sigma}n_{l-\sigma}\rangle=-i\int dE/2\pi\langle\langle d_{l\sigma}d_{l-\sigma}^{+}d_{l-\sigma},d_{l\sigma}^{+}\rangle\rangle^{<}$. In the Coulomb-blockade regime the lesser functions can be calculated according to the

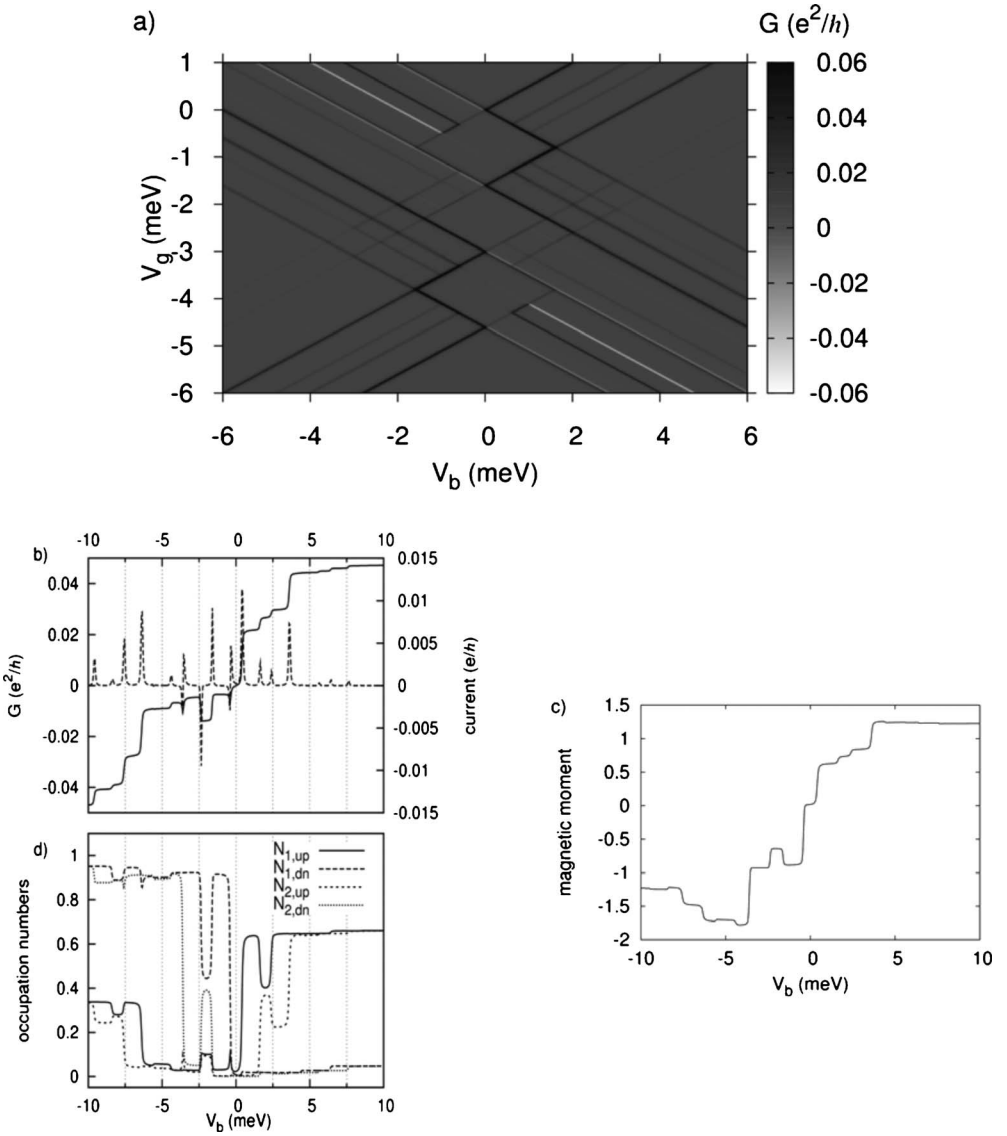

FIG. 1. (a) Differential charge conductance G versus gate and bias voltages, (b) I-V_b characteristics (solid line) and G (dashed line), (c) magnetic moment induced on the dot, and (d) occupation numbers as a function of bias voltage for V_g=0.2 meV and polarization factors: p_L=0.95, p_R=0. Parameters of the junction: ε_{10}=−0.05 meV, ε_{20}=0.55 meV, U_1=U_2=2 meV, U_{12}=1 meV, Γ=0.01 meV, and kT_L =kT_R=0.02 meV.

equation-of-motion method.[40,42] Then, $G^<_{l\sigma}$ takes a form: $G^<_{l\sigma}$=−[$(\Gamma^L_{l\sigma}f_{L\sigma}+\Gamma^R_{l\sigma}f_{R\sigma})/(\Gamma^L_{l\sigma}+\Gamma^R_{l\sigma})$]$(G^r_{l\sigma}-G^a_{l\sigma})$. Similar expression can be written for the two-particle lesser function whereas the retarded (advanced) ones are calculated from the appropriate equation of motion.[40] Finally, one obtains a set of algebraic equations for one- and two-particle occupation numbers $N_{l\sigma}$, $\langle n_{l\sigma}n_{l-\sigma}\rangle$, which are solved numerically for each value of bias voltage and temperature difference under consideration. Since the lesser Green's function is determined in terms of retarded and advanced ones, the electrical current can be written as:

$$I_\sigma = \frac{ie}{\hbar}\int \frac{dE}{2\pi}\sum_j \frac{\Gamma^L_{j\sigma}\Gamma^R_{j\sigma}}{\Gamma^L_{j\sigma}+\Gamma^R_{j\sigma}}(G^r_{j\sigma}-G^a_{j\sigma})[f_{L\sigma}(E)-f_{R\sigma}(E)] \tag{4}$$

which allows one to study transport properties.

III. ELECTRON TRANSPORT. SPIN-BLOCKADE EFFECTS

First, we assume that temperatures of both electrodes are equal T_L=T_R and study electron transport in the system subjected to the bias voltage V_b. The basic features of the charge transport through QD are well known so we focus our discussion on the system with strong spin asymmetry, in which Pauli spin blockade can be expected. Effects of spin blockade in similar systems were studied in the sequential tunneling regime with use of real-time diagrammatic technique.[28] Here, we discuss coherent transport and apply the nonequilibrium Green's function formalism. To describe the spin-blockade effects we consider a two-level quantum dot attached to external electrodes. The left electrode is a HMF with polarization factor p_L=0.95 while the right one is NM and p_R=0. The coupling strengths of both levels are the same

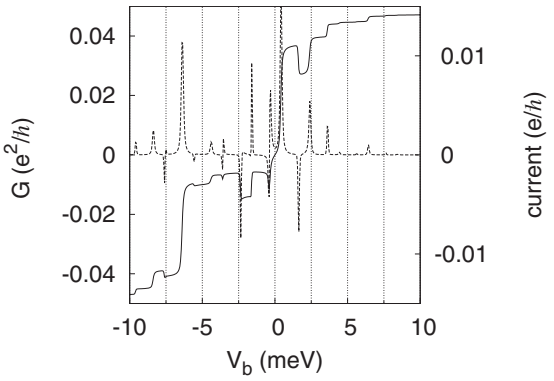

FIG. 2. I-V_b characteristics (solid line) and G (dashed line) at V_g=0.2 meV for asymmetric junction with p_L=0.95, p_R=0, and Q=0.9. Other parameters are the same as in Fig. 1.

and are equal Γ=0.01 meV. Energy levels are assumed as: ε_{10}=−0.05 meV, ε_{20}=0.55 meV. Positions of both levels can be coherently shifted with use of a gate voltage. The intralevel and interlevel correlation parameters are taken as: U_1=U_2=2 meV and U_{12}=1 meV, respectively. Studying the charge transport we assume that temperatures of both leads are equal with kT_L=kT_R=0.02 meV.

Differential charge conductance G=dI/dV_b as a function of gate voltage V_g and bias voltage V_b is presented in Fig. 1(a). Since polarization factors of both electrodes are different, $p_L \neq p_R$, the coupling strengths $\Gamma^L_{j\sigma}$ and $\Gamma^R_{j\sigma}$ also differ strongly, and the obtained patterns are more complex than typical Coulomb diamonds. For the assumed parameters the system shows negative differential conductance represented by white lines in the figure. When V_g is close to zero NDC can be observed for negative bias voltage whereas for large values of $|V_g|$ it appears for positive V_b. There is also a region of gate voltages for which blockade effects leading to NDC do not occur and current increases monotonically with increase in bias voltage. This situation takes place in the middle of the Coulomb gap with $|V_g|$ close to Coulomb parameter U=2 meV. Moreover, the conductance shows an inversion symmetry with respect to the Coulomb gap.

Spin-blockade effect is well illustrated in Figs. 1(b) and 1(d), where I-V_b characteristics, G and occupation numbers of particular states are presented for V_g=0.2 meV. For positive bias voltage electrons tunnel from the left, HMF, electrode to the right, NM, one and the current increases monotonically showing characteristic Coulomb steps. As the tunneling rate to the right lead for electrons with spin up is much lower than to the left one, these electrons start to accumulate on the dot. At first, they are located on the level 1 and then also on the level 2, which results in a large positive magnetic moment m=$N_\uparrow$−$N_\downarrow$ induced on the dot at higher values of bias voltage [Fig. 1(c)]. The situation is completely different for negative voltages, when the left, half-metallic, electrode acts as a drain. Since practically there are no states in this electrode, corresponding to spin down, electrons accumulate on the dot leading to NDC. For small V_b the current shows a sharp peak associated with a rapid increase in $N_{1\downarrow}$ from zero practically to 1 [Fig. 1(d)]. For higher voltages both levels with energies ε_1 and ε_2 are almost fully occupied with electrons of spin down. All these features, shown by the current, with negative conductance correspond to Pauli spin blockade. In general, the results are consistent with those obtained in sequential tunneling approximation[28] but the Green's function formalism applied here, allows us to take into account higher order effects, which enhance the current in the blockade regime. Such an enhancement was observed experimentally and discussed in two QDs in the cotunneling regime.[27,43] Electrons with spin up, the majority spin in the half-metallic electrode, practically do not accumulate on the dot for small reverse-bias voltage, which results in a strong negative magnetic moment induced on the dot [Fig. 1(c)]. The moment is strongly asymmetric with respect to V_b reversal.

Next, we consider transport through a molecule attached to external electrodes. In this case, coupling strengths Γ_j for two molecular levels j=1,2 can be different due to different spatial distribution of the corresponding wave functions.[44,45] To describe such a dependence, we express Γ_j in the form Γ_j=$\Gamma[1-(-1)^j Q]$. For Q=0 both levels 1 and 2 are equally coupled to electrodes whereas for $0<Q<1$ one of the levels becomes weakly coupled. Similar approach can be also applied to two QDs which are capacitively coupled and attached to external electrodes. The coupling strengths to the leads can be, then, varied for each dot separately. Assuming Q=0.9 we study influence of the level-dependent coupling strength on the results obtained in the presence of Pauli spin blockade. I-V_b characteristics and the conductance G are presented in Fig. 2 for V_g=0.2 meV. The current strongly increases in the region of small positive voltages, then, it decreases showing a significant NDC effect. It should be noted that NDC occurs both for negative and positive bias voltages. An analysis of $N_{1\sigma}$ and $N_{2\sigma}$ shows that in the region of negative voltages the main role plays Pauli spin blockade but for $V_b>0$ the NDC is of different origin. The strong suppression of the current and NDC effect can be observed when the second level, partly decoupled from electrodes enters the bias window and becomes active in the transport. The dot is then occupied by electrons with spin up coming from the half-metallic electrode. The superposition of two effects leading to NDC gives a complex I-V_b characteristics which may be observed in molecular junctions or in two dot systems.

IV. NONLINEAR THERMOPOWER

To study thermoelectric phenomena we assume that temperature of the right electrode is kept constant and equal to T_R with kT_R=0.02 meV whereas in the left electrode it is increased by ΔT so T_L=T_R+ΔT. In a presence of temperature gradient voltage V is generated and the effect is described by the Seebeck coefficient S. Usually, S is determined under the condition of vanishing charge current, I=0, and in the nonlinear-response regime, when the temperature difference ΔT between two electrodes is relatively large, one can introduce the differential thermopower defined as: S=dV/dT. In systems with magnetic electrodes, when the spin relaxation time is long enough, spin accumulation in the leads becomes important.[9,17] Temperature gradient generates, then, spin-dependent voltage V_σ=V+$\hat{\sigma}V_{spin}$ and the charge V as well as

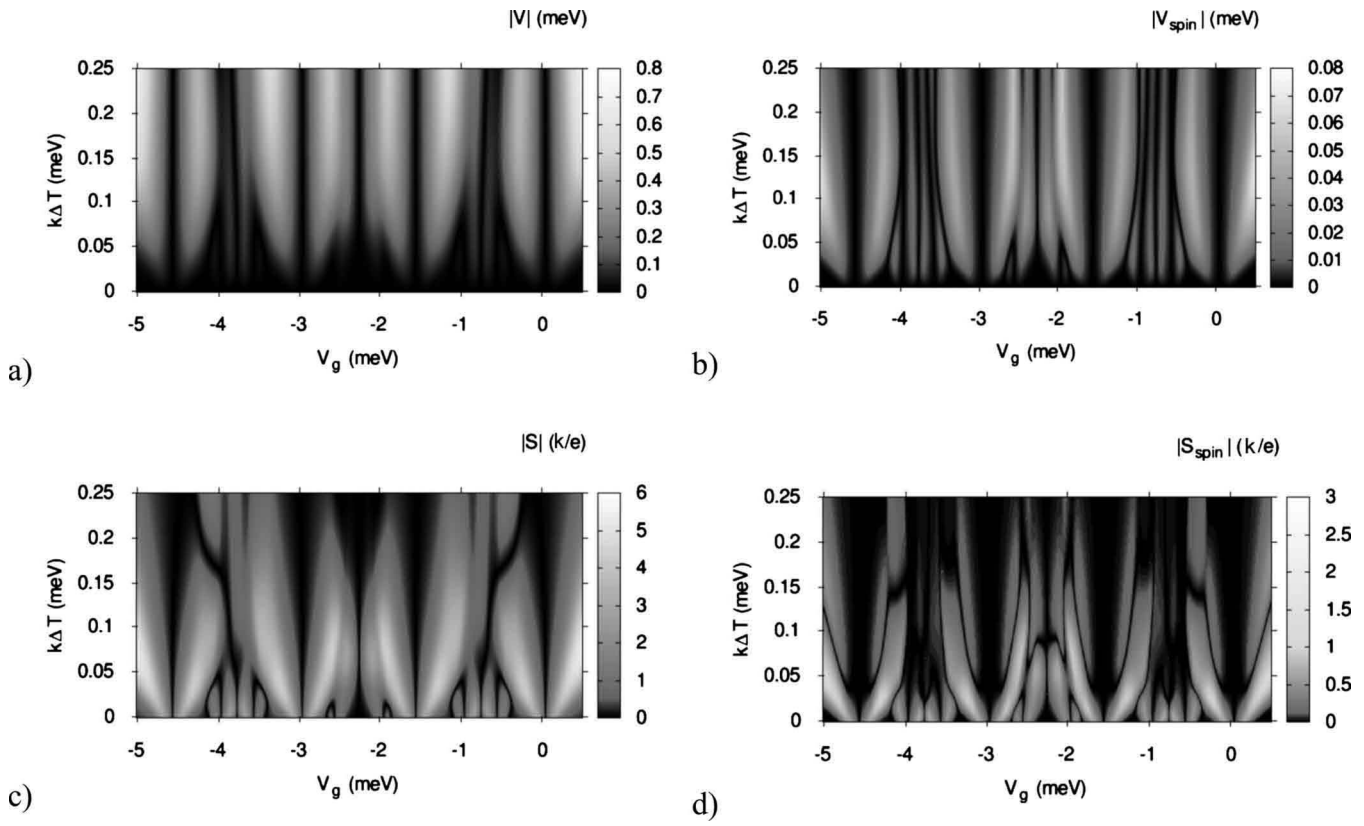

FIG. 3. (a) Charge and (b) spin voltages as well as (c) charge and (d) spin thermopower as a function of V_g and ΔT for $p_L=p_R=0.5$. Only absolute values are given. Parameters of the junction are: $\varepsilon_{10}=-0.05$ meV, $\varepsilon_{20}=0.55$ meV, $U_1=U_2=2$ meV, $U_{12}=1$ meV, $\Gamma=0.01$ meV, and $kT_R=0.02$ meV.

spin V_{spin} voltages are induced. V_σ corresponds here to the difference in electrochemical potentials of two leads in the spin channel σ. Since, the two channels are independent, the voltage V_σ and hence thermopower can be calculated under the condition of vanishing current in each spin channel, $I_\sigma=0$, or equivalently in the situation in which the charge current I and spin current I_{spin} vanish simultaneously. Therefore, for a given value of ΔT corresponding to temperature difference between electrodes the set of equations $I_\uparrow=0$, $I_\downarrow=0$ [with I_σ expressed by formula (4)] is solved numerically and generated voltages $V_\uparrow$, $V_\downarrow$ are found. After the relation $V_\sigma=V_\sigma(\Delta T)$ is determined the spin-dependent differential thermopower $S_\sigma=dV_\sigma/d(kT)$ is calculated with use of numerical procedures. One can consider the charge and spin thermopower defined by relations:[17] $S=1/2(S_\uparrow+S_\downarrow)=dV/d(kT)$ and $S_{spin}=1/2(S_\uparrow-S_\downarrow)=dV_{spin}/d(kT)$.

A. Symmetrical system

First, we study the symmetrical system with magnetic moments parallel in both electrodes and polarization factor $p_L=p_R=0.5$. The charge and spin voltages generated in the system due to temperature gradient ΔT as well as the appropriate charge and spin thermopower are depicted in Fig. 3. Since the induced voltages and thermopower strongly oscillate as a function of V_g, only absolute values are presented. Maxima (minima) appear in a vicinity of states, given by the poles of the Green's function [Eq. (3)]. If one of the states approaches the resonance, electrons tunnel due to temperature gradient giving rise to the voltage drop as well as to thermopower. When the energy level reaches the resonance the induced voltage vanishes, as currents due to electrons and holes compensate. The situation is similar for other resonant states and a number of peaks with different intensities described by the probabilities of particular one and two-particle configurations can be observed. Four resonances which correspond to levels ε_1, ε_2+U_{12}, and their Coulomb counterparts with energies $\varepsilon_1+U_{12}+U$, $\varepsilon_2+2U_{12}+U$ dominate the structure as the transport is mainly supported by these levels (see also Ref. 37). Significant changes in $|V|$ and $|V_{spin}|$ can be observed in the region of small ΔT, where the voltages rapidly increase. However, they saturate and remain practically constant for large temperature differences. With increase in temperature the levels broaden and start to overlap other, less significant, forming relatively wide bands, which dominate the whole structure [Fig. 3(a)]. On the other hand, the more rich structure can be observed for spin voltage, mainly due to the fact that generated $|V_{spin}|$ is relatively low and peaks with small intensity can be distinguished.

The charge and spin thermopower are presented in Figs. 3(c) and 3(d). One can observe that a considerable thermopower is induced in the region of relatively small ΔT. S sharply varies with V_g showing maxima (minima) in the vicinity of energy levels typical for the system. With increase in temperature peaks in vicinity of four levels, which mainly support the transport, broaden significantly as the bands are

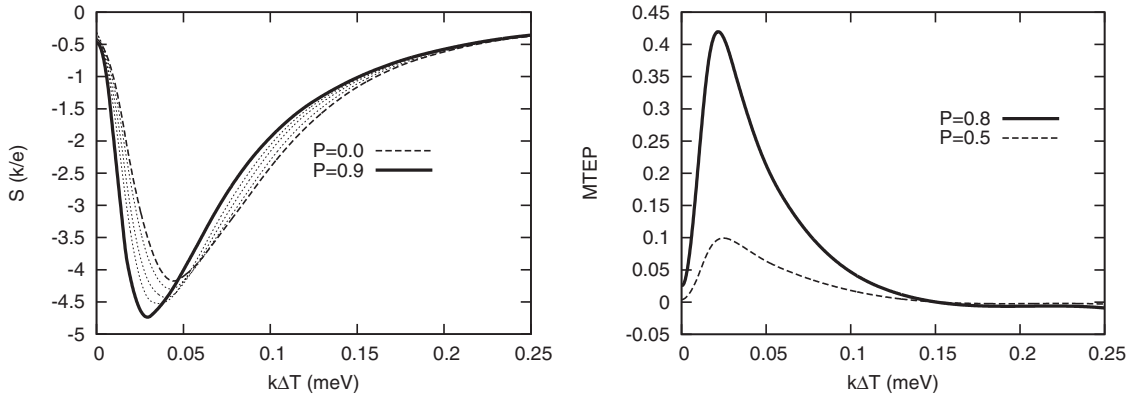

FIG. 4. (a) Charge thermopower S and (b) MTEP as a function of ΔT for several values of $p=p_L=p_R$. $V_g=-1.25$ meV. Other parameters are the same as in Fig. 3.

formed. At higher values of ΔT the thermopower decreases and regions, where S is close to zero, considerably broaden. However, for certain values of gate voltages quite significant thermopower can be still observed. A cross section taken for $V_g=-1.25$ meV is presented in Fig. 4(a). For particular gate voltage the thermopower is negative. It is also small in the limit of $\Delta T \to 0$. The chosen V_g corresponds to the situation, when Fermi level in equilibrium is lying between two states with energies ε_1+U_{12}, ε_2+U_{12} and the transport is strongly reduced at low temperatures. Absolute value of thermopower significantly increases with ΔT, achieves a narrow maximum and approaches zero for large temperature difference. Thermopower varies with polarization factor p. The most pronounced changes can be observed in the vicinity of the maximum, where $|S|$ increases with p [Fig. 4(a)]. Moreover, the curve is shifted toward smaller values of ΔT, which indicates that the generated voltage easily saturates in the system with highly polarized electrodes. It should be noted that the charge thermopower practically does not vary with p for higher temperature differences.

Thermopower S depends on the relative configuration of magnetic moments in the electrodes, and the magnetothermoelectrical power MTEP$=[S(P)-S(AP)]/S(AP)$ can be introduced. $S(P)$ and $S(AP)$ correspond here to differential thermopower determined for parallel and antiparallel configurations, respectively. MTEP calculated for symmetric junctions and two different polarization factors in electrodes is presented in Fig. 4(b). It is positive showing that $S(P)$ is greater than $S(AP)$. Moreover, MTEP strongly increases with an increase in polarization factor.

Next, we discuss spin effects in thermopower. S_{spin} in the parallel configuration calculated for different gate voltages and ΔT is presented in Fig. 3(d). Note that in the system under consideration it is possible to generate quite considerable spin thermopower, especially in the region of low ΔT. With increase in temperature difference thermopower decreases and wide regions with S_{spin} practically equal to zero can be seen. The structure of spin thermopower is complex, as it changes the sign with ΔT increasing. The cross section for $V_g=-1.25$ meV and several different polarizations are presented in Fig. 5. In the region of small ΔT spin thermopower is positive so the sign of S_{spin} is opposite to the sign of the charge thermopower, what is consistent with results obtained in the linear-response regime for a single-level dot.[17] Maximum of S_{spin} is well correlated with maximum of $|S|$. Moreover, the intensity strongly increases with leads' polarization. For high-temperature differences spin thermopower becomes negative and polarization dependence is less pronounced.

B. System with a strong spin asymmetry

Now, the junction with one HMF and one NM electrodes is investigated. Charge thermopower, generated in such a situation takes quite significant values in a wide region of ΔT. The appropriate curves, presented in Fig. 6 for two cases with HMF electrode acting as the energy source or energy drain, are relatively broad and flat. This is in contrast to symmetrical case, where $|S|$ shows a narrow maximum for small ΔT, and then decreases rather fast. In symmetric system, the state with vanishing current can be easily achieved, in which currents flowing due to temperature gradient and due to generated voltage compensate. At first, generated voltage significantly increases, but it practically saturates for small ΔT. With further increase in ΔT only very small voltage changes are necessary to keep such a state. On the other hand, in system with strong spin asymmetry, the number of

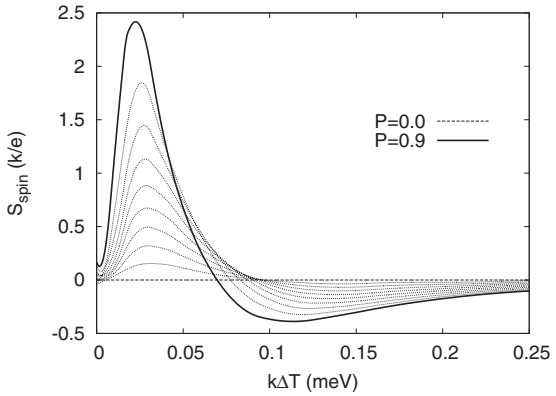

FIG. 5. Spin thermopower as a function of ΔT for several values of $p=p_L=p_R$ (polarization is varied from $p=0$ to $p=0.9$ with the step 0.1), $V_g=-1.25$ meV. Other parameters are the same as in Fig. 3.

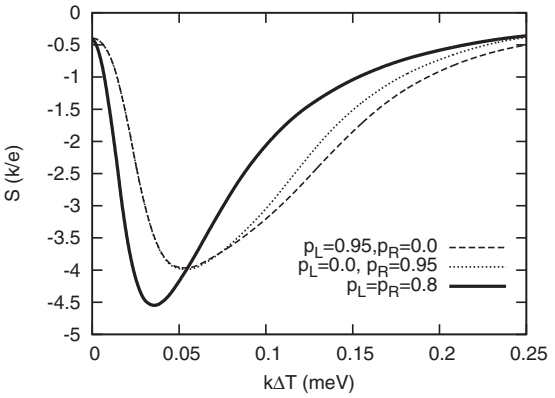

FIG. 6. Charge thermopower as a function of ΔT for symmetric and asymmetric junctions with indicated polarizations, $Q=0$. $V_g=-1.25$ meV. Other parameters are the same as in Fig. 3.

hot electrons with spin up, coming from HMF source, significantly increases with ΔT, but only a part of them can enter the NM drain electrode. To compensate this increasing electron flow, the voltage, which considerably increases with temperature, will be generated and the saturation cannot be easily obtained. It leads to a significant thermopower in a wide temperature region. Similar situation can be observed with NM electrode acting as an energy source.

Next, we discuss the behavior of spin thermopower. The appropriate curves are presented in Figs. 7(a) and 7(b). Note that S_{spin} essentially varies in the region of higher values of ΔT, if the role, which HMF electrode plays in the junction, is changed. Namely, the spin thermopower is positive in the whole temperature region for junction, in which the right electrode, with fixed temperature, is a half-metallic ferromagnet. Since NM electrode acts as an energy source, the junction is supplied with hot electrons of both spin directions. Electrons with spin up can be easily transmitted through strongly broadened by temperature, unoccupied level with energy ε_2+U_{12} and take empty states in the HMF electrode. This electron flow should be compensated due to generated voltage $V_\uparrow$. However, for higher values of ΔT, participation of holes in the transport increases. Namely, the low-lying, broadened levels, which become partially occupied can also support the transport, especially the level with energy ε_1+U_{12}. Then, the tunneling of holes will suppress the induced voltage $V_\uparrow$. On the other hand, hot electrons with spin down cannot enter the HMF electrode and they should return to the source under an influence of the induced voltage $V_\downarrow$. Voltages $V_\uparrow$ and $V_\downarrow$, which lower the electrochemical potential of the left, hot electrode are presented in Fig. 7(c). It can be observed that induced voltages differ considerably in the whole temperature region. The corresponding spin thermopower calculated as $S_{spin}=\frac{1}{2}d(V_\uparrow-V_\downarrow)/d(kT)$ slowly changes with ΔT and remains positive. When the NM electrode acts as a drain, the induced voltages do not strongly depend on spin. The generated spin thermopower is relatively small and becomes negative for higher values of ΔT [Fig. 7(a)].

Consider now the situation presented in Fig. 7(b), in which the second level becomes weakly coupled to elec-

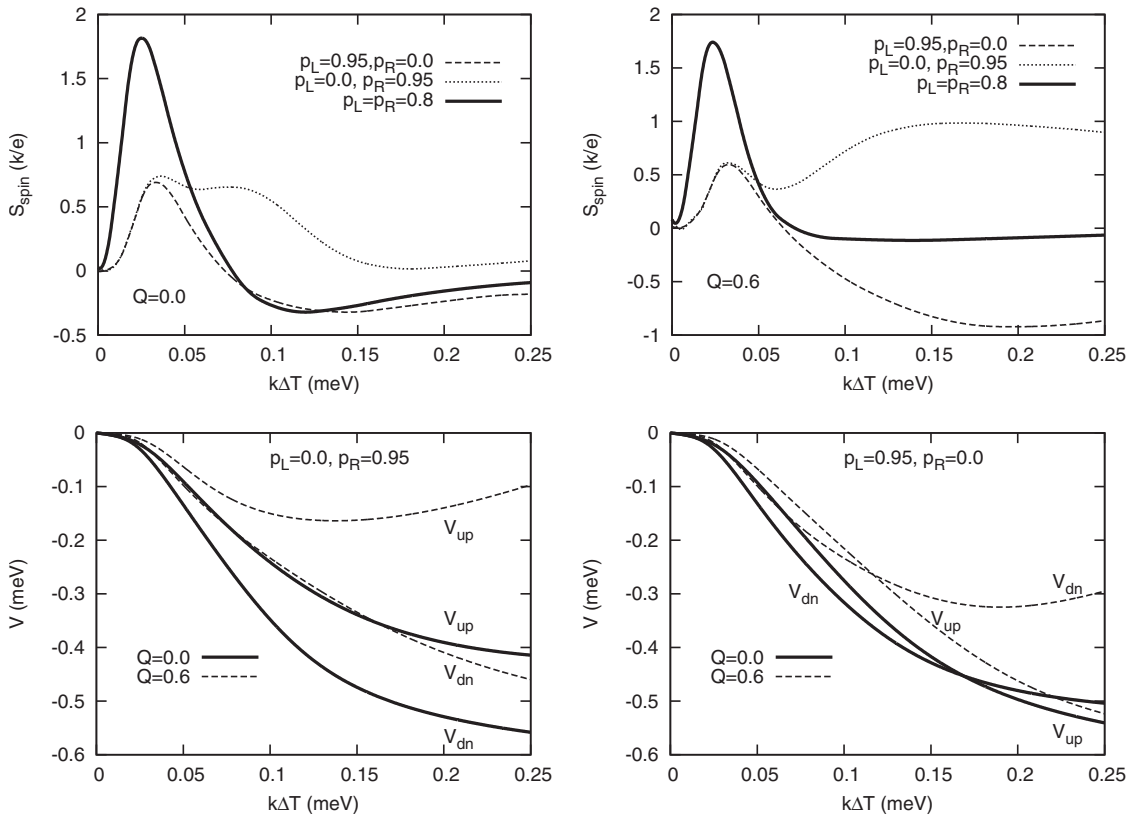

FIG. 7. [(a) and (b)] Spin thermopower and [(c) and (d)] induced spin-dependent voltage $V_\sigma=\mu_{L\sigma}-\mu_{R\sigma}$ as a function of ΔT for indicated values of polarization and Q. $V_g=-1.25$ meV. Other parameters are the same as in Fig. 3.

trodes, what corresponds to $Q \neq 0$. For symmetrical junction the spin thermopower does not considerably varies with Q. Similarly, in system with a strong spin asymmetry, changes in the spin thermopower with Q in the region of small ΔT are not very pronounced. However, different behavior can be observed for high-temperature differences. When the NM electrode acts as a source, spin thermopower starts to increase, achieving quite significant values. Transmission of hot electrons with spin up through the broadened and partially decoupled level ε_2+U_{12} is suppressed, but tunneling probability of holes increases, as the level ε_1+U_{12} is strongly coupled to electrodes. Then, the induced voltage $V_\uparrow$, which blocks the current $I_\uparrow$, is significantly suppressed [Fig. 7(c)]. On the other hand, changes in $V_\downarrow$ are weaker. Thereby, the generated voltage strongly depends on spin and a significant, positive spin thermopower arises. The different behavior can be observed if HMF electrode acts as an energy source. Though, the level ε_2+U_{12} is weakly coupled, transport through this broadened level for the majority spins does not change significantly in the region of high ΔT, as this channel is strongly supplied by the HMF hot electrode. Thereby, the generated voltage $V_\uparrow$ weakly varies with Q whereas the changes in $V_\downarrow$ are much more pronounced and $|V_\downarrow|$ strongly diminishes. It leads to a quite significant spin thermopower, which in this case is negative. Therefore, in junctions with strong spin asymmetry, containing one half-metallic electrode, spin thermopower can achieve quite significant values in the region of high ΔT and can be positive or negative in dependency on the role of this electrode. The most pronounced effect can be obtained for middle values of Q, as for large Q the level ε_2+U_{12}, nearest to the Fermi level, becomes practically decoupled from electrodes.

V. SUMMARY AND CONCLUSIONS

Studies performed in the paper for a two-level QD/molecule attached to ferromagnetic electrodes show that in such systems interesting and different features can be observed both in electron and energy transport. The analysis of I-V_b characteristics shows that NDC effect due to Pauli spin blockade can be obtained in junctions with one HMF and one NM electrodes, which is consistent with result found in the sequential tunneling regime.[28] NDC appears, then, for the forward or reverse bias in dependency on the gate voltage. However, if the level with higher energy is weakly coupled to electrodes, more complex characteristics can be obtained and NDC occurs for both bias polarizations, generated by two different mechanisms.

Thermoelectric phenomena in a two-level QD/molecule attached to ferromagnetic electrodes are also interesting. First of all, in systems with symmetrical junctions significant charge and spin thermopower can be generated. Spin effects are the most pronounced in the region of small ΔT, where both charge and spin thermopower increase with leads' polarization. Moreover, magnetothermoelectric power can be observed, indicating that, similarly to charge transport, thermopower is suppressed in systems with antiparallel orientation of magnetic moments.

Spin asymmetry of the junction due to the presence of one HMF electrode enhances thermopower in the region of higher values of ΔT. Spin thermopower strongly varies in this temperature region, if the role of half-metallic electrode is changed from the energy source to the energy drain. The most interesting is the case when the HMF electrode acts as charge or energy drain. In both cases electrons with spin down emitted by NM source cannot enter the HMF electrode due to the lack of spin-down states so they must accumulate on the dot or return to the source. When the bias voltage V_b is applied to the junction, electrons mainly accumulate on the dot leading to Pauli spin blockade. In a presence of temperature gradient electrons with spin down will return to the NM source giving rise to a considerable spin thermopower. The effect can be especially pronounced in the molecular junctions or two-dot systems with one of the levels (dots) weakly coupled to the leads. Temperature gradient applied to the junction in such a way that HMF electrode acts as an energy drain will generate a significant spin voltage. Thereby, the system could be considered as an effective spin battery, which would allow to convert the heat into spin voltage in spintronic devices.

[1] A. I. Hochbaum, R. Chen, R. D. Delgado, W. Liang, E. C. Garnett, M. Najarian, A. Majumdar, and P. Yang, Nature (London) **451**, 163 (2008).
[2] K. Baheti, J. A. Malen, P. Doak, P. Reddy, S. Y. Jang, T. D. Tilley, A. Majumdar, and R. A. Segalman, Nano Lett. **8**, 715 (2008).
[3] P. Reddy, S. Y. Jang, R. A. Segalman, and A. Majumdar, Science **315**, 1568 (2007).
[4] G. Joshi, H. Lee, Y. Lan, X. Wang, G. Zhu, D. Wang, R. W. Gould, D. C. Cuff, M. Y. Tang, M. S. Dresselhaus, G. Chen, and Z. Ren, Nano Lett. **8**, 4670 (2008).
[5] M. Christensen, A. B. Abrahamsen, N. B. Christensen, F. Juranyi, N. H. Andersen, K. Lefmann, J. Anderasson, C. R. H. Bahl, and B. B. Iversen, Nature Mater. **7**, 811 (2008).
[6] E. McCann and V. I. Fal'ko, Phys. Rev. B **66**, 134424 (2002); **68**, 172404 (2003).
[7] L. Gravier, S. Serrano-Guisan, F. Reuse, and J. P. Ansermet, Phys. Rev. B **73**, 024419 (2006).
[8] L. Gravier, S. Serrano-Guisan, F. Reuse, and J. P. Ansermet, Phys. Rev. B **73**, 052410 (2006).
[9] K. Uchida, S. Takahashi, K. Harii, J. Ieda, W. Koshibae, K. Ando, S. Maekawa, and E. Saitoh, Nature (London) **455**, 778 (2008).
[10] Z.-C. Wang, G. Su, and S. Gao, Phys. Rev. B **63**, 224419 (2001).
[11] M. Hatami, G. E. W. Bauer, Q. Zhang, and P. J. Kelly, Phys. Rev. B **79**, 174426 (2009).
[12] M. Hatami, G. E. W. Bauer, Q. Zhang, and P. J. Kelly, Phys. Rev. Lett. **99**, 066603 (2007).
[13] K. M. D. Hals, A. Brataas, and G. E. W. Bauer, Solid State Commun. **150**, 461 (2010).

[14] O. Tsyplyatyev, O. Kashuba, and V. I. Fal'ko, Phys. Rev. B **74**, 132403 (2006).
[15] M. Krawiec and K. I. Wysokinski, Phys. Rev. B **73**, 075307 (2006).
[16] Y. Dubi and M. Di Ventra, Phys. Rev. B **79**, 081302 (2009).
[17] R. Świrkowicz, M. Wierzbicki, and J. Barnaś, Phys. Rev. B **80**, 195409 (2009).
[18] C. W. J. Beenakker and A. A. M. Staring, Phys. Rev. B **46**, 9667 (1992).
[19] X. Zianni, Phys. Rev. B **75**, 045344 (2007).
[20] M. Tsaousidou and G. P. Triberis, *28th International Conference on the Physics of Semiconductors ICPS 2006*, AIP Conf. Proc. No. 893 (AIP, New York, 2007), p. 801.
[21] J. Koch, F. von Oppen, Y. Oreg, and E. Sela, Phys. Rev. B **70**, 195107 (2004).
[22] M. Turek and K. A. Matveev, Phys. Rev. B **65**, 115332 (2002).
[23] R. Scheibner, H. Buhmann, D. Reuter, M. N. Kiselev, and L. W. Molenkamp, Phys. Rev. Lett. **95**, 176602 (2005).
[24] J. Iñarrea, G. Platero, and A. H. MacDonald, Phys. Rev. B **76**, 085329 (2007).
[25] J. Fransson and M. Rasander, Phys. Rev. B **73**, 205333 (2006).
[26] B. Muralidharan and S. Datta, Phys. Rev. B **76**, 035432 (2007).
[27] I. Weymann, Phys. Rev. B **78**, 045310 (2008).
[28] I. Weymann and J. Barnaś, J. Phys.: Condens. Matter **19**, 096208 (2007).
[29] K. Hamaya, M. Kitabatake, K. Shibata, M. Jung, S. Ishida, T. Taniyama, K. Hirakawa, Y. Arakawa, and T. Machida, Phys. Rev. Lett. **102**, 236806 (2009).
[30] D. Segal, Phys. Rev. B **73**, 205415 (2006).
[31] N. Zeng and J. S. Wang, Phys. Rev. B **78**, 024305 (2008).
[32] R. Scheibner, M. Konig, D. Reuter, A. D. Wieck, C. Gould, H. Buhmann, and L. W. Molenkamp, New J. Phys. **10**, 083016 (2008).
[33] J. P. Bergfield and C. A. Stafford, Phys. Rev. B **79**, 245125 (2009).
[34] M. Krawiec and K. I. Wysokinski, Phys. Rev. B **75**, 155330 (2007).
[35] M. Leijnse, M. R. Wegewijs, and K. Flensberg, Phys. Rev. B **82**, 045412 (2010).
[36] C. M. Finch, V. M. Garcia-Suarez, and C. J. Lambert, Phys. Rev. B **79**, 033405 (2009).
[37] M. Wierzbicki and R. Świrkowicz, J. Phys.: Condens. Matter **22**, 185302 (2010).
[38] Y. Meir, N. S. Wingreen, and P. A. Lee, Phys. Rev. Lett. **70**, 2601 (1993).
[39] H. Haug and A.-P. Jauho, *Quntum Kinetics in Transport and Optics of Semiconductors* (Springer, Berlin, 1996).
[40] Y. C. Chang and D. M.-T. Kuo, Phys. Rev. B **77**, 245412 (2008).
[41] D. M.-T. Kuo and Y. C. Chang, Phys. Rev. Lett. **99**, 086803 (2007).
[42] C. Niu, D. L. Lin, and T. H. Lin, J. Phys.: Condens. Matter **11**, 1511 (1999).
[43] K. Ono, D. G. Austing, Y. Tukura, and S. Tarucha, Science **297**, 1313 (2002).
[44] M. H. Hettler, H. Schoeller, and W. Wenzel, Europhys. Lett. **57**, 571 (2002).
[45] A. Thielmann, M. H. Hettler, J. Konig, and G. Schon, Phys. Rev. B **71**, 045341 (2005).